CHROM. 23 274

High-performance liquid chromatography of amino acids, peptides and proteins

CXIV[a]. Protein interactions with porous coulombic sorbents: comparison of experimental findings with predictions of several adsorption models

A. JOHNSTON and M. T. W. HEARN*

Department of Biochemistry and Centre of Bioprocess Technology, Monash University, Clayton, Victoria 3168 (Australia)

ABSTRACT

   The adsorption behaviour of three anion-exchange sorbents, DEAE Trisacryl M, DEAE Sepharose FF and DEAE Fractogel 650 M has been investigated for proteins of different size and charge distribution. The maximum capacity, q_m, and the dissociation constant, K_d, were found to be protein size dependent. Protein loadings with carbonic anhydrase infer unhindered access to the pores of these three sorbents and thus high capacities. Kinetic profiles, monitoring protein uptake from solution, indicated that the rate of adsorption was fast for small proteins. Mathematical models, derived by others, were adopted to extract values for the interaction rate, k_1, and the effective diffusion, D_p. The simplest model of Horstmann *et al.* [*J. Chromatogr.*, 361 (1986) 179] gave high values for k_1, confirming that this model lumped together the resistances to mass transfer. Correlation between theory and experiment was best when using the most sophisticated model, that of Arve and Liapis [*AIChE. J.*, 33 (1987) 179] where the resulting values for k_1 were larger. Diffusion for the smaller proteins agreed well with bulk diffusion, indicating little restriction to mass transfer through the pores. Contrary to this, values of D_p for the largest protein, ferritin, were 1/40th of the free diffusivities, further highlighting the influence of protein size on pore accessibility.

INTRODUCTION

   The structural diversity and dynamic nature of proteins give rise to a plethora of species that differ widely in physical, chemical and biological properties. For a particular protein, microheterogeneity can arise from natural evolution, during transcription and post-translational modifications, or from misoccurances during isolation. With the onsurge of recombinant DNA technology, biosynthetically derived protein heterogeneity has become increasingly more prevalent and of greater concern at both the recovery and quality control stages of product manufacture. The existence

---

[a] For Part CXIII, see ref. 45.

of isoforms of proteins, differing in a number of properties such as charge distribution, apparent size and three dimensional structure, has thus fostered the need for careful and highly tuned separation techniques that selectively purify the desired protein from its contaminants, and in particular contaminants that are closely related structurally.

In laboratory-scale purifications, affinity chromatography is one such technique used, despite its relative cost per cycle. However, the increasing demand for recombinant proteins with human therapeutic, industrial, diagnostic or other commercial uses has necessitated the need to process large quantities of source material. Further steps other than immuno-affinity or other forms of biospecific chromatographic procedures are therefore essential in the overall mass separation at the preparative process scale. In particular, tandem steps are usually chosen to maximize the throughput of the source material to minimize time and to achieve a high level of purity. This last criterion becomes more important when the protein is designated for human therapeutic use. As an example of this strategy, the scheme chosen for the extraction of serum albumin from human plasma entailed taking a volume reduction step first, namely ion-exchange chromatography, whilst the most expensive step, affinity chromatography, was used last, to ensure 99% purity at minimum cost [1]. This scheme thus follows two of the six cardinal rules in the heuristics of process design [2].

Positive chromatographic purification can be simply visualised as entailing three operational steps. (1) The starting material is loaded onto a column packed with adsorbent resin and the target protein is specifically adsorbed; (2) the column is washed with running buffer to remove unwanted, unadsorbed components; (3) the target protein, having adsorbed to the resin during step (1) is desorbed with an appropriate elution buffer. These steps are fundamental to all modes of process chromatography, and are widely used in practice today to purify important therapeutic protein substances from biological fluids and fermentation broths. Optimization of these steps has up till now concentrated on the process parameters, such as flow-rate and loadability. However, it has recently been shown that the mechanism of protein interaction needs to be considered as an integral part of the process optimisation [3]. For example, the performance of the resin with respect to its interactive properties can affect the stability of the protein and its purification. At a process level, effects such as slow diffusion of the protein through the porous network, tortuosity, non-specific adsorption onto heterogeneous sites and rotational masking can become detrimental to process efficiency. In addition, adsorption of the target protein to the chromatographic resin may cause undesirable structural changes to the protein. With reversed-phase sorbents, for instance, the highly hydrophobic surface has been found to promote unfolding of the protein [4–7]. Reorientation of immunoglobulin G (IgG) bound to an ion-exchange sorbent has also been observed [8]. Essentially, the hydrophobic and coulombic forces that are important in maintaining protein structure are the same forces often used to affect chromatographic separations. In conjunction with the adverse effects of interaction with the resin, the elution buffers used to desorb the protein, such as organic solvents in the case of reversed-phase, or high salt concentrations in ion-exchange chromatography, can also promote conformational change or aggregation of the protein molecules [8–10]. Thus, exposure of the protein to buffers vastly different in composition to those it experiences in its natural physiological environment may cause a perturbance in the protein's integrity and ultimately result in a loss of activity.

It is therefore clear that the time the protein takes to pass down the column (the column residence time) interacting with the resin along its path, desorbing and resorbing from buffer to resin is crucial [11]. Residence time depends upon the kinetic rate and strength of the interaction, as well as the rate at which the protein diffuses to the functional groups distributed on the surface of the resin. Porous resins, offering a high surface area and high capacity, are commonly used in chromatographic separations. In preparative procedures, the choice of large macroporous resins is preferred over non-porous sorbents due to higher productivity without sacrificing resolution and column back pressure. Protein diffusion through the porous matrix of the resin then becomes an additionally important time-dependent factor. The rate constant, indicative of the kinetics of adsorption, and the effective diffusivity of the protein are thus two physicochemical parameters that characterize retention and hence are important parameters governing process performance. Unfortunately these two parameters cannot be measured directly from experimental work. Recent research has been directed towards developing mathematical models that describe the adsorption process from which these physicochemical parameters can be calculated. The applicability and adequacy of each of these models will depend upon the complexity of the crude source mixture, the integrity of the target protein and the homogeneity of the resin's macro- and micro-structure.

In this paper, the adsorption behaviour of several proteins in the ion-exchange mode has therefore been examined, in order to assess the adequacy of several models prominent in literature. Two ion-exchange resins, in industrial employment and a new synthetic ion-exchange resin are evaluated both in terms of the kinetic rate constant and the apparent rate of protein diffusion through the porous resins.

THEORY

Langmuir isotherms

The adsorption of protein to interactive resins was initially perceived as being similar to the adsorption of gases and small molecules to surfaces. The adsorbent is visualized as having a number of identical, non-cooperative sites, upon which a monolayer coverage of the protein adsorbs. The dependence of the amount of the protein that adsorbs (at constant temperature and after a certain time interval) at a particular solution concentration is called the adsorption isotherm. The simplest type of isotherm, the Langmuir isotherm, is based on the principles of stoichiometry, with one protein molecule interacting with one specific functional site. The expression thus derived takes the form

$$q^* = \frac{K_a \, q_m \, c^*}{1 + K_a \, c^*} \tag{1}$$

The parameters K_a and q_m can be calculated from a double reciprocal plot of eqn. 1 ($1/c^*$ against $1/q^*$) where under ideal operational criteria, this plot is predicted to be linear. This Langmuir isotherm has been found to adequately describe, for example, the affinity adsorption of IgG to immobilized Protein A on Superose [12], and of bovine serum albumin to Cibacron Blue Sepharose CL-6B [23]. Reports based on low concentration loading onto a non-porous sorbent also demonstrate that the Langmuir

approach provides a realistic interpretation of other types of adsorption processes [14]. The adsorption behaviour of other affinity systems have also been tailored to fit empirical relationships, like the Freundlich isotherm. Yang *et al.* [15] have demonstrated this correlation with the binding of trypsin to trypsin inhibitor immobilized to Sepharose 4B.

The utility of the Langmuir isotherm is however limiting. The association constant, K_a, reflecting the strength of the interaction, and the maximum capacity, q_m, are *equilibrium* parameters and shed no light on the *rate* of interaction. The adsorption of the protein to the functional groups on the sorbent is a dynamic process requiring the movement of the protein from the bulk mobile phase to the stationary phase. In process chromatography, where large volumes of dilute protein concentrations are processed, the time taken for equilibrium to be achieved is significant. It is therefore inappropriate to use a model equation that assumes that equilibrium is established instantaneously at all points surrounding the particle's external and internal surface. Thus a model describing the time-dependency of the protein concentration should be used.

The model according to Horstmann et al. [16]

Horstmann *et al.* [16] have therefore proposed that the protein adsorbs to a porous resin at a rate k_1, and that this rate is equal to the rate of disappearance of the protein from solution less the rate of desorption from the resin. The concentration of the protein in solution at any time can then be described by,

$$C(t) = C_0 - v \frac{(b + a)\left\{1 - \exp\left[-2a\left(\frac{v}{V}\right)k_1 t\right]\right\}}{\left(\frac{b + a}{b - a}\right) - \exp\left[-2a\left(\frac{v}{V}\right)k_1 t\right]} \tag{2}$$

In the derivation Horstmann *et al.* [16] have assumed the concentration in the bulk solution is constant, that is there is no stagnant film layer surrounding the resin particles, so that there is no film mass transfer resistance. In addition, there is no concentration gradient within the pores of the particles, and no diffusional restrictions to the protein movement, so that the diffusion of protein is assumed to be equal to the bulk diffusivity. Thus, this model uses a single mass transfer parameter, k_1, to describe the adsorption of protein to sorbent. The equation is based on a bimolecular-type second order reversible interaction, and in the limit of high k_1, the adsorption process can be assumed to be irreversible (that is, desorption from the resin is negligible).

The model according to Arnold et al. [17]

Arnold *et al.* [17] have found, however, that if the protein is large and the pore openings of the sorbent small, then the rate at which the protein diffuses into the pores of the resin is significantly retarded. In the case of high affinity adsorption such as ion-exchange chromatography, the rate of interaction is concomitantly fast, and its contribution to the overall rate of adsorption considered negligible. In this case, the overall rate of protein uptake from bulk solution is said to be limited by protein

diffusion into the pores of the particles. The interactive process in this situation can be represented by the expression,

$$D_p \frac{(1 - e)\, t}{r_p^2 e} = \frac{1}{3} \ln \left| \frac{\alpha^3 + \omega^3}{\alpha^3 + 1} \right| + \frac{1}{6\alpha} \ln \left[\frac{(\alpha^2 - \alpha + 1)(\alpha + \omega)^2}{(\alpha^2 - \alpha\omega + \omega^2)(\alpha + 1)^2} \right] +$$

$$\frac{1}{3^{1/3}\alpha} \left[\arctan \left(\frac{2 - \alpha}{3^{1/3}\alpha} \right) - \arctan \left(\frac{2\omega - \alpha}{3^{1/3}\alpha} \right) \right] \qquad (3)$$

This equation may be applied to any batch adsorption process that has essentially a fast irreversible rate of adsorption. The above expression assumes that the bulk concentration at the pore entrance and the intraporous concentration are equivalent, that is, there are no film diffusion effects contributing to the protein movement into the pores. In addition the volume held in the pore volume is small compared with the volume of the bulk volume. These assumptions are similar to those adopted by Horstmann et al. [16], except that in deriving eqn. 3 it is assumed that the pore diffusivity is the rate determining step, whilst the dynamics of the interaction are ignored, since for an irreversible adsorption, $k_2 \to 0$ and $k_1 \to \infty$.

The model according to Tsou and Graham [18]

Distribution of the protein in the bulk solution surrounding the resin particle, however, may not necessarily be uniform due to concentration gradients. These may be minimized or eliminated by adequate agitation. Moderately high agitation, however, may still not eliminate these gradients in the neighbourhood of the particles, rendering a resistance to mass transfer which is manifested by a film layer. Tsou and Graham [18] have developed a model equation based on the two phase diffusion model, which allows for two effective resistances, one dependent on the film mass transfer of the protein through the film layer and the other related to the diffusion of the protein into the porous resin. The overall rate is then defined as being proportional to an overall mass transfer coefficient, K, and an equilibrium parameter, m'', which are both assumed to remain constant over the range of protein concentration usually encountered in adsorption processes. This implies that the adsorption is limited to the linear part of the adsorption isotherm, so that the kinetic solution becomes,

$$\ln\, (1 - F(t)) = \frac{-3\, K\, t}{r_p} \left(\frac{v}{V} + \frac{1}{m''} \right) \qquad (4)$$

Eqn. 4 is simplified by considering situations where the film mass transfer is infinitely fast and under these conditions it can be assumed that $1/m'' \ll v/V$ and the mass transfer coefficient, K, is governed by pore diffusion, D_p, thus establishing a simple linear relationship between $\ln\, (1 - F(t))$ and D_p. Like eqn. 3, eqn. 4 implies that the overall rate of adsorption is solely proportional to the rate at which the protein diffuses through the resin, and that the rate of interaction is negligible, that is the dynamics of the interaction are again ignored.

The model according to Arve and Liapis [19]

From theoretical consideration many cases of protein adsorption can be contemplated where the rates of interaction, diffusion and mass transfer across the film are comparable, such that eqns. 2, 3 and 4 do not adequately describe the adsorption process. Indeed from practical considerations this may always be the circumstance. Discrimination between the rates has always been a difficult task experimentally, hence the need to make certain assumptions about which step is the rate limiting step. Various investigators [20–23] and most recently, Arve and Liapis [19], have taken on the formidable task of developing sophisticated models that incorporate parameters which describe three mass transfer resistances. The fundamental mass balance equations, such as those given in eqn. 5 have yet to be solved analytically, but by making various assumptions, one can arrive at solutions, such as those given by Horstmann *et al.* [16], Tsou and Graham [18] and Arnold *et al.* [17]. Arve and Liapis [19], amongst others, have adopted numerical techniques, to arrive at solutions to the equations, that take into account three mass transfer resistances. The bulk phase concentration is taken to be uniform, except for a small film layer around the particle surface, and once equilibrium is achieved the concentration adsorbed to the resin can be described by the Langmuir isotherm, eqn. 1. The batch adsorption model presented by Arve and Liapis [19] for the protein–ligand interaction of an irreversible process (presumed to incorporate very high affinity interactions, like ion-exchange) has been evaluated here, in which k_1 represents an irreversible rate constant. According to their numerical solution, the overall rate is assumed to be dictated by a combination of the film mass transfer coefficient, K_f, the pore diffusivity, D_p, and the interaction rate, k_1. A detailed description of the coupled partial differential equations can be found in the literature [19], but for the purpose of reference, eqn. 5 is given here to represent the rate of change of the bulk concentration as proposed by Arve and Liapis [19], thus,

$$\frac{\partial C(t)}{\partial t} = f\left(K_f,\, D_p,\, k_1,\, e,\, r_p,\, e_p,\, q_m,\, C_0\right) \tag{5}$$

These models, represented by eqns. 2–5, have been developed to quantify the physicochemical parameters associated with batch adsorption. Equilibrium isotherms, designed to reflect the static performance of a sorbent, have been used over the last decade in protein adsorption studies. However, the information from the isotherm alone cannot yield estimates of the rates at which protein adsorbs, and indeed for an irreversible adsorption process such as ion-exchange, in which the isotherms are often rectangular in shape, very little information can be extracted. Therefore kinetic equations, such as eqns. 2–5, which describe the mechanism of adsorption in terms of rate limiting steps have been selected to illucidate the dynamic nature of adsorption behaviour. The models reported above make the same assumptions with regard to parameter independence on protein concentration and bulk diffusivity in batch systems, with the following differences. (1) The model of Horstmann *et al.* [16] which is based on a kinetically controlled batch adsorption. (2) The model of Arnold *et al.* [17] which assumes an irreversible adsorption with pore diffusion controlling the rate of adsorption. (3) The model of Tsou and Graham [18] which consider both film and pore diffusion to be rate controlling. (4) The model of Arve and Liapis [19] which

incorporates film and pore diffusion, as well as the kinetic rate into the overall rate of adsorption.

The models to date have neglected to discriminate secondary equilibrium effects, such as protein–protein interactions, protein-ion equilibrium and non-equilibrium effects. This is because of the increased complexity involved in solving mass balance equations that describe non-ideality. This neglect may be acceptable if one is to predict and optimize the purification of a "well behaved" and "well characterized" protein. The manufacture of novel macroporous packing materials, that have minimal diffusional restrictions and improved flow properties, also assists in ensuring near ideal adsorption. On the other hand, the discovery of more synthetic and natural protein variants, proof of multiple orientation and conformational changes during adsorption, and requirement for extreme levels of protein purity, places more demand on better parameter estimation during process optimization.

EXPERIMENTAL

Proteins with low isoelectric points have been selected, so that adsorption to anion-exchange media at near neutral pH is possible. Human serum albumin (HSA), as a 21% solution, was kindly donated by Commonwealth Serum Laboratories (C.S.L.) (Melbourne, Australia). Carbonic anhydrase, from *Saccharomyces cerevisiae*, and ferritin, from horse liver (chromatographically isolated) were purchased from Sigma (St. Louis, MO, USA). A 5 mM disodium–dihydrogen orthophosphate buffer was chosen, with a pH corresponding to 1 to 2 units above the pI of the target protein, in the case of ferritin and HSA (pH 6), whilst pH 11.5 was necessary for carbonic anhydrase. Buffer salts were obtained from Aldrich (Milwaukee, WI, USA). Three weak ion-exchange resins were used: a polymethacrylate resin, DEAE Trisacryl M, purchased from Australia Chemical Company (Melbourne, Australia), DEAE Fast Flow Sepharose, an industrially important agarose resin and a gift from C.S.L., and the polymeric DEAE Fractogel 650 M, from Merck (Darmstadt, Germany). Experimental apparatus for batch adsorption, included a Model 2238 UV Spectrophotometer and a Model 2210 two pen chart recorder from Pharmacia (Uppsala, Sweden). Pascal and Fortran programs were written on an IBM PC with linkage to a VAX mainframe, to generate theoretical solutions outlined in the theory section. Experimental data was also analysed using the IBM PC. Each experiment for measuring the isotherm was performed a minimum of three times to ensure reproducibility, and three kinetic profiles were used to extract the physicochemical parameters associated with eqns. 2–5, using linear regression or a least square determination. Thus the values listed in Tables IV and V are average values of three separate experimental runs.

Values for the film mass transfer coefficient, K_f, were taken from the correlation of Ohashi *et al.* [24] whilst an initial estimate for the pore diffusivity, D_p, was taken to be the value for the mobile free diffusivity determined from the correlation given by Young *et al.* [25].

RESULTS AND DISCUSSION

In the present study, the three proteins (HSA, ferritin and carbonic anhydrase)

TABLE I

PROPERTIES OF THE ANION-EXCHANGE RESINS

Resin	Particle size (μm)[a]	Capacity; albumin (mg/ml)	Ionic capacity (meq/ml)	Exclusion limit (relative molecular mass)
DEAE Sepharose FF	45–165	110[b]	100	4 000 000
DEAE Fractogel 650 M	45–90	20–30[c]	100	5 000 000
DEAE Trisacryl M	40–80	100–110[d]	300	10 000 000

[a] Wet bead diameter.
[b] Determined in 0.05 M phosphate buffer pH 9.0, Pharmacia specification.
[c] Determined in 0.05 M phosphate buffer pH 7.0, Merck specification.
[d] Determined in 0.05 M Tris–HCl buffer pH 8.0, LKB-Pharmacia specification.

were selected on the basis of size and isoelectric point, to principally assess the affect of protein hydrodynamic volume on (1) the capacity of the anion-exchange resins and (2) the rate of adsorption to the functional groups on the resins. Table I lists the physical properties of the proteins, in terms of their molecular masses, their hydrodynamic radii, derived from correlation data [26], their pI and their free or bulk diffusivity in solution, also derived from correlated data [25]. The resins are all weak anion exchangers, with the functional group being diethylaminoethyl (DEAE), and vary in their physical properties and their adsorption capacities, see Table II. According to the manufacturer's specifications, and others [27], the Trisacryl M and the Sepharose FF resins have similar capacity for HSA, although Trisacryl M has a higher ionic capacity in terms of meq/ml resin, as well as having a smaller mean particle size (hence larger surface area) and a greater exclusion limit (larger pore size). Fractogel 650 M, like Sepharose FF has a high ionic capacity, however, this sorbent has been specified by the manufacturers to have a low capacity for HSA, with a low exclusion limit.

   In this study, the dynamic capacity of these resins was measured using a bath system as previously described [28] whereby a protein solution was injected into a well mixed bath containing buffer and resin and the uptake of the protein was monitored continuously. Serial injections were carried out until the resin no longer adsorbed the protein from solution, this being exhibited by a steady-state UV absorbance reading of the on-line spectrophotometer. The total protein adsorbed was calculated from the difference between the total amount added to the bath and that remaining in solution. From the experimental results of each injection, adsorption isotherms were thus constructed, reflecting the equilibrium capacity of the sorbent at a particular concentration of the protein in solution.

TABLE II

PROPERTIES OF THE PROTEINS

Protein	Molecular mass	Radius (nm)	pI	Bulk diffusivity ($\times 10^{-11}$ m^2/s)
Ferritin	440 000	8.4	4.0	3.2
Human serum albumin	67 000	4.5	4.9	6.1
Carbonic anhydrase	30 000	3.5	6.0	7.9

Equilibrium studies

Fig. 1a and b shows the experimental data for the adsorption of HSA and ferritin to the various weak ion-exchange resins. Fig. 1a shows that the Trisacryl M and Sepharose FF have high capacities for HSA, whilst Fractogel 650 M exhibits a lower value, as expected from the reported values in Table I. The opposite trend is true for ferritin, where the maximum capacity found experimentally, q_m, for Trisacryl M is 3-fold lower than Fractogel 650 M, despite the fact that Trisacryl M has a higher ligand density, and larger exclusion limit. This trend has previously been documented by Kato *et al.* [27] in an extensive study of the protein capacity of commercial anion exchangers. This result suggests that mechanisms other than simple point surface charge interactions are dominating the adsorption of ferritin to these weak ion exchangers. It is well known that proteins form dimers and trimers in solution, and that protein stacking onto affinity adsorption sorbents can occur [29]. Multilayering of the protein onto the ion-exchange resin is thus a possible explanation for this observed trend.

Adsorption isotherms were also obtained for the smallest protein, carbonic anhydrase. The values of q_m found experimentally and q_m and K_a obtained from double reciprocal plots ($1/q^*$ *versus* $1/c^*$, refer eqn. 1) for this protein, together with those for HSA and ferritin are given in Table III. This table clearly shows that the capacity of a particular resin is dependent on the size of the protein. Comparing the protein capacity of the Trisacryl M, that for the smallest protein, carbonic anhydrase (radius = 3.5 nm) was the greatest, $q_m = 2.7\ \mu$mol/ml, compared to $q_m = 0.05\ \mu$mol/ml for ferritin (radius = 8.4 nm), consistent with carbonic anhydrase having the greatest accessibility to the functional groups in the interior of the resin. Porous particles have
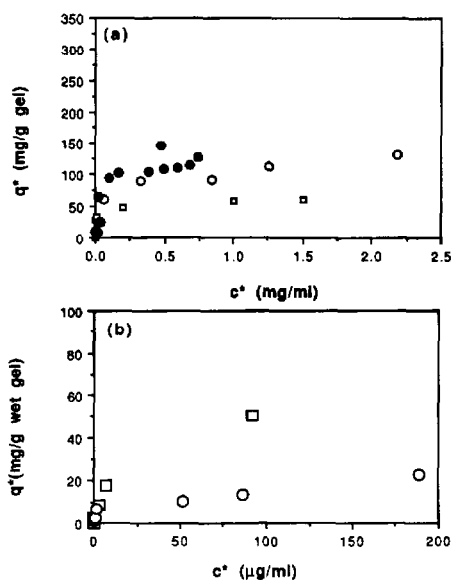

Fig. 1. Adsorption isotherms for the binding to the weak anion-exchange resins. (a) HSA, (b) ferritin. ○ = DEAE Trisacryl M; ● = DEAE Sepharose FF; □ = DEAE Fractogel 650 M.

TABLE III

VALUES OBTAINED FROM THE EQUILIBRIUM EXPERIMENTS

Resin	q_m (mg/g)		q_m (μmol/ml) Experimental	K_a		Coefficient of regression
	Theoretical	Experimental		ml/mg	$\times 10^6$ M^{-1}	
HSA						
Trisacryl M	99.7	140	2.1	56	3.8	0.978
Sepharose FF	64.0	110	1.6	12	0.8	0.999
Fractogel 650 M	48.9	55	0.8	40	2.7	0.933
Ferritin						
Trisacryl M	19	—	0.04	377	165	0.997
Fractogel 650 M	75	—	0.18	95	40	0.999
Carbonic anhydrase						
Trisacryl M	35.1	35	2.7	140	4.2	0.991

an appreciable portion of these ligand groups within the particle. The same trend is apparent for Fractogel 650 M where q_m is 5-fold greater for the smaller HSA than for ferritin. It should be kept in mind, however, that the capacity of an ion-exchange resin depends on the extent of ionization of the functional groups on the resin as well as the apparent charge of the protein, both of which are a function of the pH and ionic strength of the buffer. Therefore the high capacity for carbonic anhydrase may be indicative of the higher pH of the buffer (pH 11.0) rather than solely due to the relatively small size of the protein. Irrespectively, the relationship between capacity, accessibility and pore restriction has been confirmed by these results, as well as substantially documented by a number of other investigators [18,30 33].

For the conditions shown in Fig. 1 and in other cases not plotted here, the isotherms are rectangular in shape and the data do not fit the Langmuir equation, eqn. 1. However, in order to fit the theoretical models, it has been necessary to use eqn. 1 to calculate the association constant K_a, the results of which are given in Table III. For further discussion of the relationship of K_a in the "irreversible" adsorption of proteins in ion-exchange chromatography, see Horstmann *et al.* [16]. The rectangular nature of the experimental isotherms of Fig. 1a and b indicates very high association constants (where the initial slopes of the isotherms are proportional to this constant) which is to be expected since the interaction is dominated by strong electrostatic forces. The high values for K_a, 10^6–10^7 M^{-1}, compare well with values reported in the literature, for example the association constant for bovine serum albumin binding to Sephadex A50 [18] was $K_a = 2.2 \cdot 10^6$ M^{-1}. These K_a values are an order of magnitude greater than the association constants for biospecific affinity adsorption, for example the adsorption of the protein α-chymotrypsin to proflavin immobilised to Lichrospher 500 has reported [34] to be $0.15 \cdot 10^6$ M^{-1}. These calculated association constants, like the capacity, also appear to be protein size dependent. The largest protein, ferritin, shows K_a values of the order of 10^7 M^{-1}, whilst that for carbonic anhydrase is only 10^6 M^{-1}. Results from zonal elution chromatography of carbonic anhydrase onto Mono Q, reporting a low retention coefficient and early elution in gradient elution, confirm the weak interaction exhibited

by carbonic anhydrase with anion-exchange sorbents [35]. Multiple factors underly the relationship between K_a and molecular size and it is not possible in these preliminary results to ascribe a particular molecular or physical feature as the sole origin of this effect. The association of the protein with the ionic resin is predominantly electrostatic, the strength of this association is dictated by the charge anisotropy of the protein, the number and spatial arrangement of the charges and its distance from the resin. Whilst models, such as the net charge model [36], have been introduced to predict the retention characteristics of proteins in high-performance ion-exchange chromatography, it has been found that proteins do adsorb to anion-exchange resins below their pI value [35,37–39] because of a non-uniform distribution of surface charge. Thus, the interaction is more complex than one charged species adsorbing to an ionic surface, and hence the strength of this interaction, K_a, is not predictable from an analysis solely based on net charge considerations or size criteria.

Although the parameters, q_m and K_a, are equilibrium parameters, and give no indication of the rate at which the protein adsorbs to the resin, they nevertheless represent the adsorption condition after extended periods of time. Using these static equilibrium parameters, one can therefore predict time-averages of the dynamic adsorption parameters. Eqn. 2 of the model of Horstmann *et al.* [16] and the numerical solution of the model of Arve and Liapis [19], for example, use these equilibrium values in the calculation of the interaction rate constant. The dynamic adsorption of protein to ion-exchange resin was therefore investigated for the three proteins, HSA, ferritin and carbonic anhydrase by measuring the rate of protein uptake from solution, the results of which are presented below. The shape of the curve reflects, amongst other things, the strength of the interaction and the overall rate of interaction. Its curvature will vary according to the level of saturation of the sorbent. At low concentrations, for example <0.1 mg/ml of HSA, the three resins studied here will not be near saturation (see the isotherms of Fig. 1) and uptake of the protein from solution will generally be fast in the case of an ion-exchange interaction. The ionic adsorption at this level is also irreversible, with $C(t)/C_0$ approaching zero. This pattern is in contrast to affinity adsorption, in which the interaction is not as strong, the adsorption is incomplete, and equilibrium is established after longer periods of time. Kinetic adsorption curves of HSA binding to Cibacron Blue F3GA-Fractogel HW75 [33] and IgG to Protein A-Superose B [16] have shown figures of $C(t)/C_0$ asymptoting to 0.45 and 0.3, respectively. At high concentrations, >0.5 mg/ml of HSA for example, the resins used in this study are near saturation and the kinetic curve should therefore reflect this by asymptoting to a non zero $C(t)/C_0$.

Kinetic studies

Fig. 2 compares the dimensionless concentrations of HSA, ferritin and carbonic anhydrase adsorbing to the weak anion resins Trisacryl M, Sepharose FF and Fractogel 650 M as a function of time. These plots show that the resins Trisacryl M and Fractogel 650 M exhibit similar kinetic profiles, whilst those of Sepharose FF are different. In addition, it can be seen that the adsorption of the small protein, carbonic anhydrase, yields kinetic profiles that approach zero quickly (steady-state time is 10 min) indicating that the protein is irreversibly bound to the resin and that the resin is far from saturation. Adsorption of HSA to Trisacryl M and Fractogel 650 M also show similar behaviour. Binding of HSA to the Sepharose FF, however, is indicative of
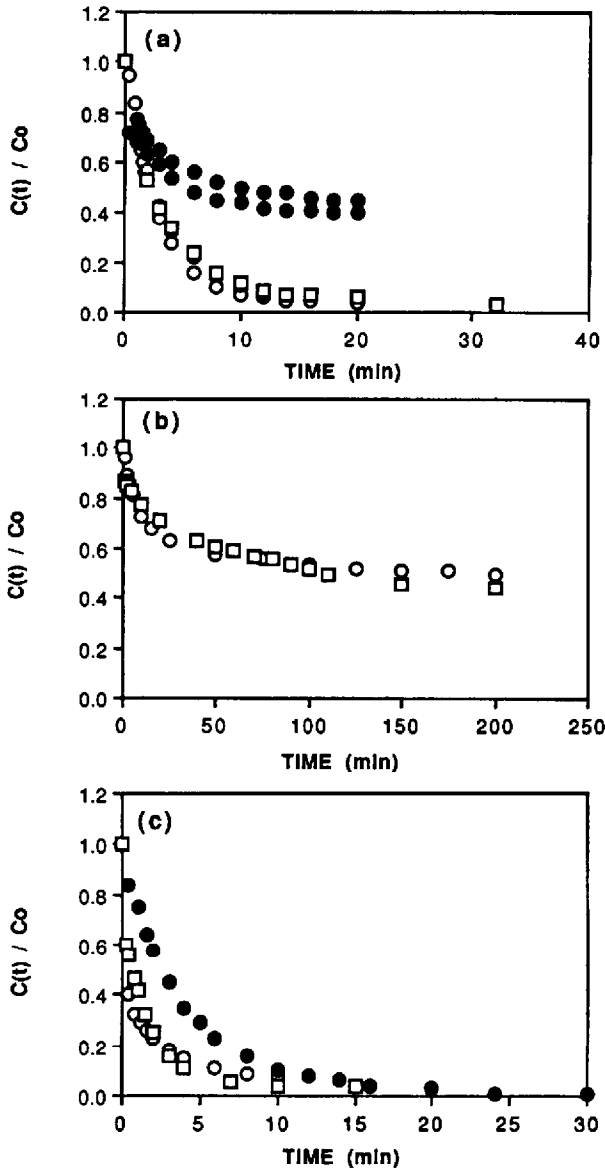
Fig. 2. Kinetic profiles for the adsorption to the weak anion-exchange resins. (a) HSA, (b) ferritin, (c) carbonic anhydrase. ○ = DEAE Trisacryl M; ● = DEAE Sepharose FF; □ = DEAE Fractogel 650 M.

a reversible interaction, with $C(t)/C_0$ approaching 0.4. The association constant found from serial injections, is also lower than that for Trisacryl M and Fractogel 650 M which concurs with a lower affinity. The adsorption of ferritin to all the resins also does not approach zero, $C(t)/C_0 = 0.4$, see Fig. 2b, and this might be attributed to the high concentration of protein initially injected into the bath, C_0 here being 0.1 mg/ml, with
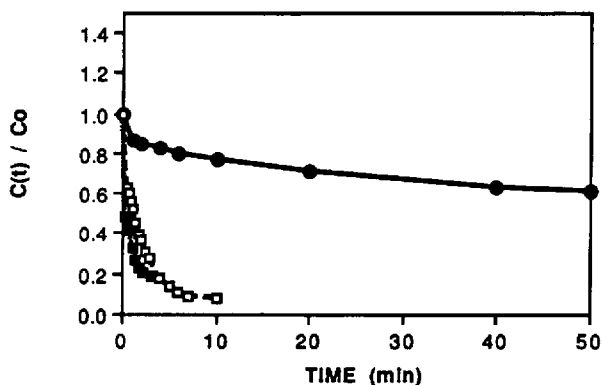
Fig. 3. Kinetic profiles for the adsorption of the proteins to DEAE Trisacryl M. ● = Ferritin; □ = HSA; ■ = carbonic anhydrase.

the equilibrium concentration, c^*, becoming 0.04 mg/ml, which is near saturation of the resins (see Fig. 1b).

Fig. 3 compares, at constant molar concentration, the adsorption behaviour of the three different proteins to Trisacryl M. These results directly relate how the size of the protein influences the overall rate of the adsorption. Interaction with an ion-exchange resin, is influenced by a combination of things, of which the contact area of the protein ligand interaction is just one. It can be expected, however, that a large protein with a large global surface area may have a stronger interaction with the charged resin, and hence larger K_a value. However, from unit cell packing considerations, the number of proteins able to interact per unit adsorption area of the sorbent will be limited because of steric hindrance. It is thus not surprising then that the adsorption profiles of Fig. 3, shows $C(t)/C_0$ approaching 0.4 for the large protein ferritin, and that in the experimental system studied, equilibration time was greater than 50 min.

Modelling studies

The kinetic profiles presented above illustrate qualitative differences in the adsorption behaviour of different weak ion-exchange resins with three proteins of different molecular masses and different surface charge distribution. However, in order to extract quantitative values for the rate of interaction, and the diffusion coefficient, an iteration procedure and regression analysis involving the theoretical equations presented in the theory section is required. Utilising the models of Horstmann *et al.* [16], Arnold *et al.* [17], Tsou and Graham [18] and Arve and Liapis [19], the results of the adsorption experiments have been compared with predictions of these four models. The findings are given below.

Data evaluation using the model of Horstmann et al. [16]. Eqn. 2 of Horstmann *et al.* [16] has been used to generate the theoretical profiles illustrated in Fig. 4. Non-linear regression has been used to determine the value of k_1 for the curve of best fit. Fig. 4a is an example of a case where sum of squares of variances (representing the goodness of fit) is low, of the order of 10^{-4}. The adsorption of low concentrations of HSA (<0.1 mg/ml) to all of the resins studied showed good correlation between
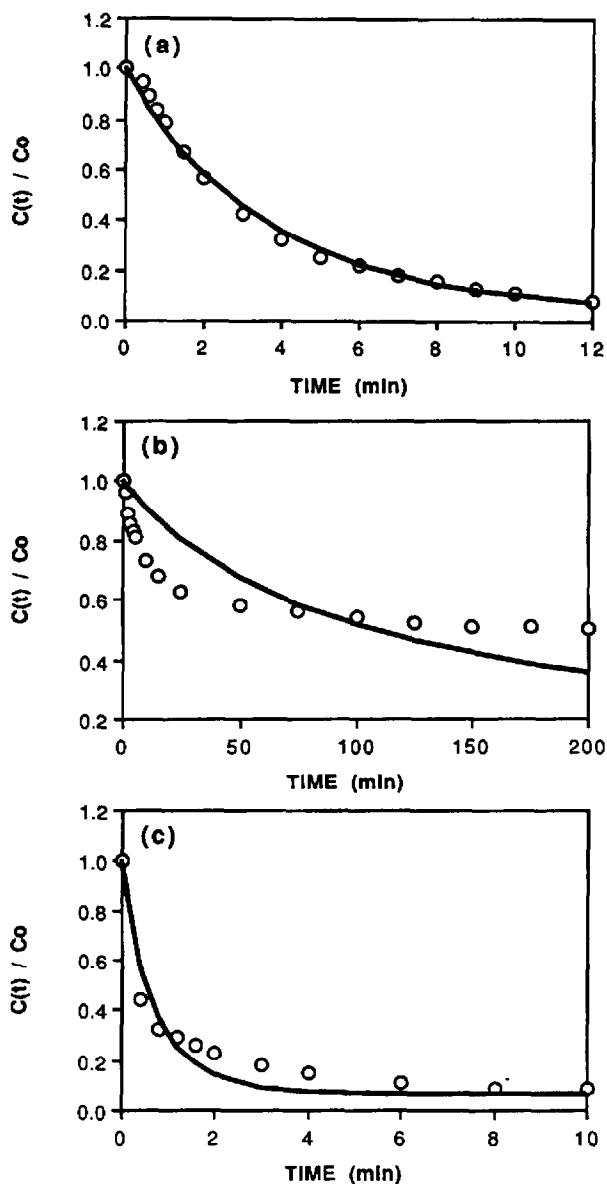
Fig. 4. Typical kinetic profiles for the adsorption to DEAE Trisacryl M. $C_0 = 104$ $\mu g/ml$. (a) HSA, $k_1 = 0.007$ ml/mg s; (b) ferritin, $k_1 = 0.002$ ml/mg s; (c) carbonic anhydrase, $k_1 = 0.127$ ml/mg s. $\bigcirc$ = Experimental; —— = eqn. 2.

experiment and theory. Converse to this, at higher concentrations (>0.5 mg/ml), and for the large protein, ferritin, the fit was poor, with the sum of squares being 10^{-2}, Fig. 4b. In all cases the regression analysis was designed to provide the minimum sum of residuals, such that the best fit in the case of Fig. 4b gave a theoretical curve that crossed the experimental curve. In retrospect, it may have been more appropriate to fit

the last part of the curve, so that the theoretical and experimental curves attained the same equilibrium position. However, it should be kept in mind that the model of Horstmann *et al.* [16] has not been developed for ion-exchange adsorption. This model has been derived from a stoichiometric assumption that one protein molecule adsorbs to one functional group on the resin. In its derivation, it has also inherently assumed that the rate of adsorption is the rate limiting step. For large proteins, diffusional restrictions into small pores will be significant, so that the predicted equilibrium position, or $C(t = \infty)$ of ferritin in Fig. 4b is likely to be lower than that attained experimentally.

Data evaluation using the model of Arnold et al. [17]. The parameters g, (proportional to the maximum capacity) and $D_p (1 - e)/(r_p^2 e)$ as defined by the model of Arnold *et al.* [17], eqn. 3, were varied to generate curves of best fit for the experimental profiles, shown as Fig. 5. The theoretical curve of Fig. 5a appears to fit the experimental curve best near equilibrium, whilst Fig. 5b, HSA binding to Sepharose FF, is illustrative of the case where the correlation between theory and experimental is poor at all times. As has been already shown, the Sepharose FF resin behaves differently from the other resins (see Figs. 2, 5b and 6a). The observed behaviour might be attributed to the heterogeneity of the resin, due to a large size
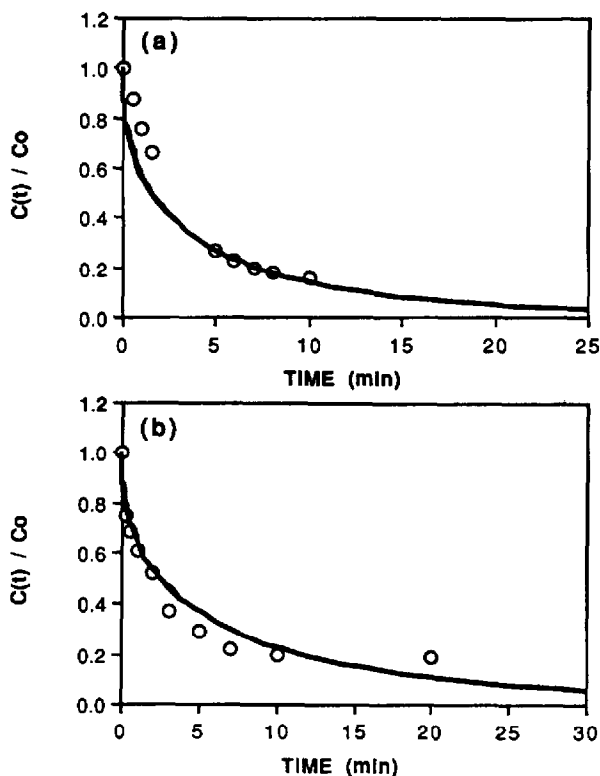

Fig. 5. Typical kinetic profiles for the adsorption of HSA to weak anion-exchange resins. (a) DEAE Trisacryl M, $C_0 = 65$ μg/ml, $D_p = 0.5 \cdot 10^{-11}$ m^2/s. (b) DEAE Sepharose FF, $C_0 = 93$ μg/ml, $D_p = 1.3 \cdot 10^{-11}$ m^2/s. $\bigcirc$ = Experimental; — = eqn. 3.

distribution (45–165 μm) and a large pore size distribution. In addition, eqn. 3 has been derived for the case of irreversible adsorption, which means that all the protein from solution should be adsorbed to the resin until the resin itself becomes completely saturated. Thus the model predicts each time that $C(t)/C_0$ approaches zero, although experimentally this is not always the case. Hence the parameters extracted from this model may not have any real physical significance.
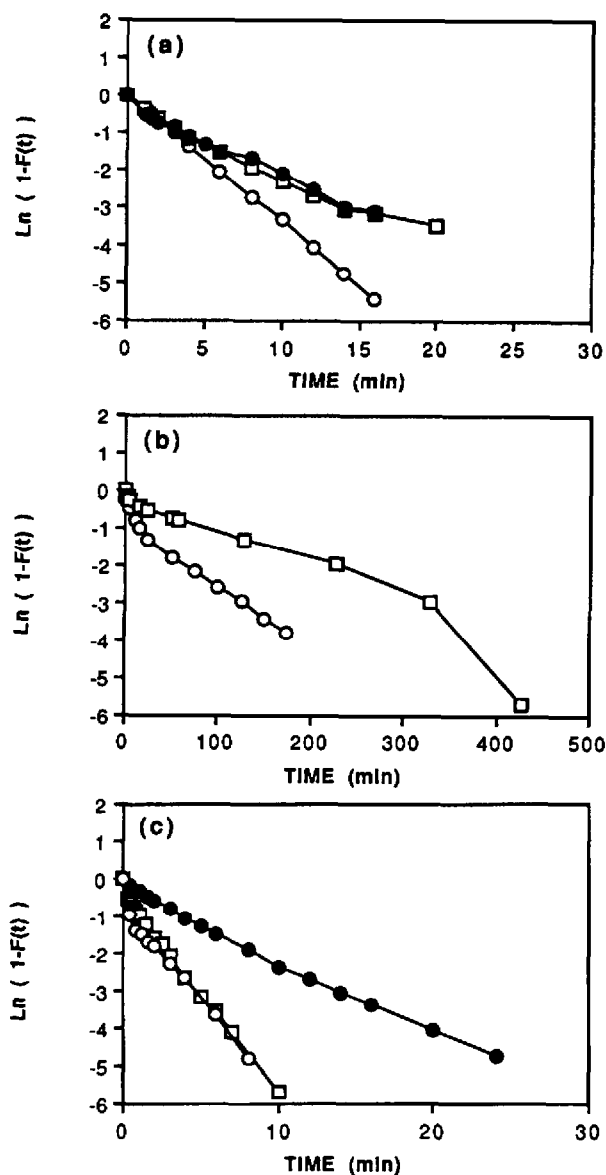

Fig. 6. Typical logarithmic transformations from eqn. 4. $C_0 = 104$ μg/ml. (a) HSA, (b) ferritin, (c) carbonic anhydrase. $\bigcirc$ = DEAE Trisacryl M; $\bullet$ = DEAE Sepharose FF; $\square$ = Fractogel 650 M.

Data evaluation using the model of Tsou and Graham [18]. Logarithmic transformations of the adsorption profiles, according to eqn. 4, are illustrated in Fig. 6. According to Tsou and Graham [18], if the adsorption is governed by pore diffusion, then these plots should be linear. Straight lines were seen to occur for low concentrations of the smaller proteins, HSA and carbonic anhydrase adsorbing to all resins studied, although two slopes were evident for ferritin (Fig. 6a). Similarly, at high concentrations (> 1 mg/ml) near saturation of the sorbent, there is a significant change in the slope of the plots of ln $[1 - F(t)]$ *versus* time, t, and biphasic behaviour is apparent. This change in the slope of the logarithmic plots might correspond to the transfer of protein mobility from film diffusion to pore diffusion, according to eqn. 4. At low concentrations, a component of the initial slope corresponding to the film diffusion may be so small that it is not detected, with the apparent slope reflecting the pore diffusion. Use of this model may therefore be limited, since at high concentration of the protein the adsorption isotherm is no longer linear, and the slope of the operating line, m'', changes with the concentration. The concentration of protein within the pores may also be significant, establishing concentration gradients, that may have some effect on the linearity of the plots of ln $[1 - F(t)]$ *versus* time.

Despite the divergence from linearity, the plots of Fig. 6 illustrate differences between the resins. The Sepharose FF resin demonstrates slower rates, manifested in these logarithmic plots as smaller slopes, and the faster binding of ferritin to Trisacryl M than to Fractogel 650 M is clearly evident.

Data evaluation using the model of Arve and Liapis [19]. A 20% deviation of the film mass transfer coefficient, K_f, (varying in the radius of the resin particle, the porosity, and the bulk diffusivity) was found to have little affect on the shape of the concentration profile, allowing only a two parameter curve fitting exercise for the model of Arve and Liapis [19]. Thus, iteration of the parameters D_p and k_1 according to this model led to the theoretical curves of Fig. 7. The curve of ferritin binding to Fractogel 650 M, Fig. 7b, is indicative of low concentration profiles, with the theoretical curve agreeing well with the experimental profile. This has found to be the case for the majority of the experimental curves of low concentrations of HSA adsorbing to the Trisacryl M and Fractogel 650 M resins, with the coefficient of regression being greater than 0.9 in all cases. At low concentrations, adsorption is not at saturation levels and the mechanism of interaction is likely to be less complex. Lower regression coefficients, 0.7–0.8, were calculated for the experiments with high concentrations of HSA, where the system is at or near saturation of the sorbent, and non-equilibrium effects, such as protein–protein interaction, and other non-ideal effects such as steric hindrance may be more significant. Other theoretical predictions, given in Fig. 7b, designed to provide the best fit to the adsorption of HSA to Sepharose FF, also showed a poor correlation between theory and experimental. In Fig. 7b, the model of Arve and Liapis predicts that all the protein adsorbs to the resin, $C(t)/C_0 = 0.0$, whereas, as Figs. 2a and 5b show, this is not the case. Poor fits were also apparent for adsorption of carbonic anhydrase, yet good fits were obtained for all the ferritin experiments.

In terms of interpretation of the experimental data, this model appears to be the most useful of those previously described, for it takes into account the mass transfer resistance, represented as K_f, and the diffusive restrictions of the protein into the interior of the particles, D_p, in the determination of the interaction rate constant, k_1.
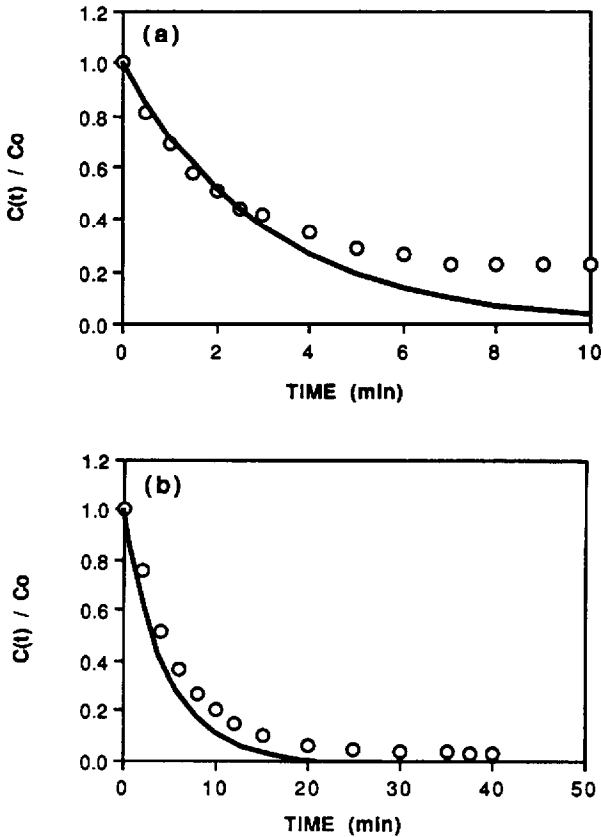
Fig. 7. Typical kinetic profiles for the adsorption to weak anion-exchange resins. (a) HSA binding to DEAE Sepharose FF, $C_0 = 56 \, \mu g/ml$, $K_f = 5 \cdot 10^{-6} \, m/s$, $r_p = 52.5 \, \mu m$, $D_p = 6.1 \cdot 10^{-11} \, m^2/s$, $k_1 = 1.0 \, ml/mg \, s$. (b) Ferritin binding to DEAE Fractogel 650 M, $C_0 = 248 \, \mu g/ml$, $K_f = 2.5 \cdot 10^{-6} \, m/s$, $r_p = 34 \, \mu m$, $D_p = 0.9 \cdot 10^{-12} \, m^2/s$, $k_1 = 0.5 \, ml/mg \, s$. $\bigcirc$ = Experimental; — = eqn. 5.

The theoretical profiles therefore represent the sum contribution of the series of resistances to the overall rate of adsorption.

Comparison of the kinetic data. In Fig. 8, direct comparison is made of the theoretical profiles of Horstmann *et al.* [16], Arnold *et al.* [17] and the numerical calculation of Arve and Liapis [19]. The model of Tsou and Graham (eqn. 4) cannot be easily transformed into a kinetic profile of concentration with time. The experimental conditions of the adsorption of a 0.1 mg/ml solution of HSA to the resins Trisacryl M, Fig. 8a, and Fractogel 650 M, Fig. 8b, and of ferritin to Fractogel 650 M, Fig. 8c), are given also. The shape of the curves generated from the model of Arve and Liapis show the best fit to the experimental profiles, and this was found to be the case in the majority of experiments undertaken. In these cases, the plots asymptote to zero, and are not as steep at the onset of adsorption. This is not surprising since a two parameter curve fit is possible.

From the theoretical curves presented in the Figs. 1–8 and other experimental data, the relevant physicochemical parameters, D_p and k_1, have been calculated and
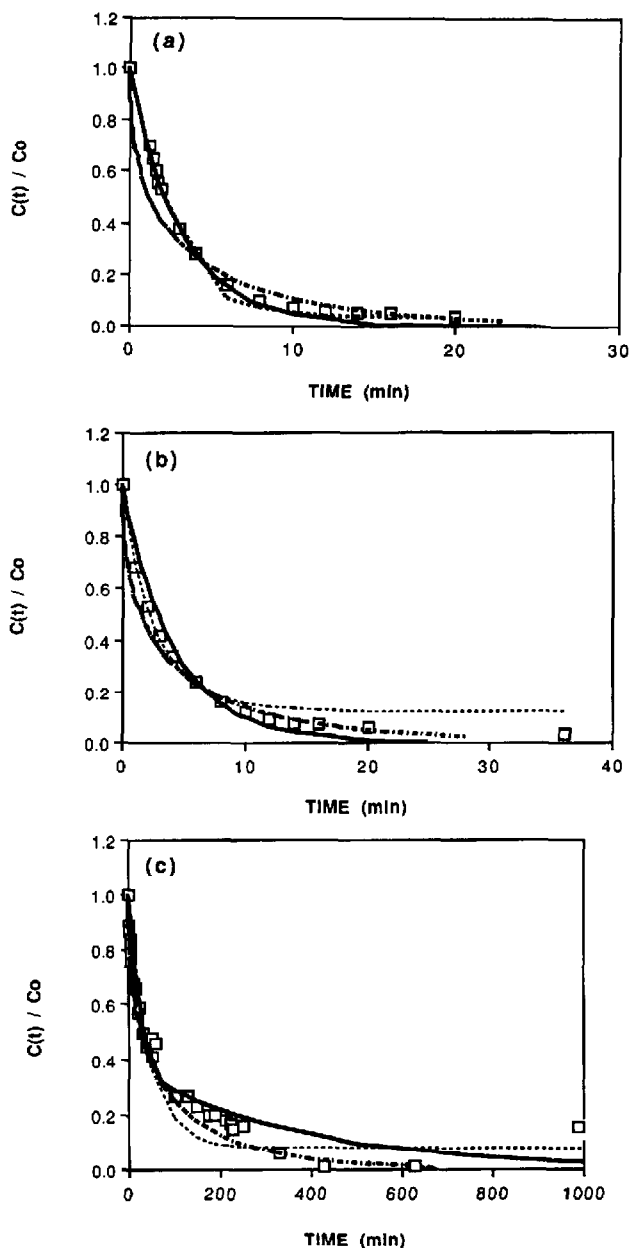
Fig. 8. Comparison of the theoretical curves obtained from eqns. 2–5. $C_0 = 104$ µg/ml. (a) □ = HSA binding to DEAE Trisacryl M, ------ = eqn. 2 of Horstmann et al. [16], $k_1 = 0.008$ ml/mg s, –··–·– = eqn. 3 of Arnold et al. [17], $D_p = 0.6 \cdot 10^{-11}$ m²/s, ——— = simulation of Arve and Liapis [19], $k_1 = 0.5$ ml/mg s, $D_p = 6.1 \cdot 10^{-11}$ m²/s. (b) □ = HSA binding to DEAE Fractogel 650 M, ------ = eqn. 2 of Horstmann et al. [16], $k_1 = 0.002$ ml/mg s, –··–·– = eqn. 3 of Arnold et al. [17], $D_p = 0.13 \cdot 10^{-11}$ m²/s, ——— = simulation of Arve and Liapis [19], $k_1 = 0.5$ ml/mg s, $D_p = 6.1 \cdot 10^{-11}$ m²/s. (c) □ = Ferritin binding to DEAE Fractogel 650 M, ------ = eqn. 2 of Horstmann et al. [16], $k_1 = 0.001$ ml/mg s, –··–·– = eqn. 3 of Arnold et al. [17], $D_p = 4.7 \cdot 10^{-11}$ m²/s, ——— = simulation of Arve and Liapis [19], $k_1 = 0.1$ ml/mg s, $D_p = 0.3 \cdot 10^{-11}$ m²/s.

TABLE IV

KINETIC PARAMETERS FROM THE MODEL EQUATIONS

Resin	C_0 (μg/ml)	k_1 (ml/mg s)		D_p ($\times 10^{-11}$ m^2/s)			
		Eqn. 2	Eqn. 5	Eqn. 2	Eqn. 4	Eqn. 5	Eqn. 3
Trisacryl M	56 ± 7	0.012 ± 0.033	0.02	6.1	7.3 ± 0.2	6.1	0.9 ± 0.2
	104 ± 1	0.007 ± 0.001	0.01	6.1	5.2 ± 0.3	6.1	0.9 ± 0.2
Sepharose FF	55 ± 12	0.011 ± 0.002	1.0	6.1	18 ± 5	6.1	3.12 ± 1.8
	104	Not found	0.3	6.1	11	6.1	2.59
Fractogel 650 M	51	0.120 ± 0.039	0.3	6.1	8.4	6.1	2.4
	104	0.002	0.5	6.1	5.1 ± 0.5	6.1	1.3

the results are listed in Tables IV and V. Table IV shows a comparison of the adsorption parameters from the binding of HSA to the three resins, Trisacryl M, Sepharose FF and Fractogel 650 M, at two different concentrations. Table V compares the parameters for the three different proteins.

(i) Examination of k_1. It has been previously reported [33] that the values obtained from the model of Horstmann *et al.* [16] overestimate the value for k_1, as the model does not discriminate between the other steps involved with the overall adsorption rate. Use of this model may only be appropriate and physically consistent in the case where the protein to pore size ratio is small, as in the adsorption of carbonic anhydrase to the Trisacryl M resin. Furthermore, Arve and Liapis [19] have provided evidence that the model of Horstmann *et al.* [16] is thermodynamically inconsistent. Therefore, if this model equation is used in estimating the interaction rate, k_1, in other cases, for example HSA binding to Fractogel 650 M or ferritin to Trisacryl M, the value may be up to an order of magnitude too low [k_1 (Horstmann *et al.*) = 0.067, k_1 (Arve and Liapis) = 0.014]. This has been found to be the case in previous work [33]. The interaction rates k_1 from the model of Horstmann *et al.* [16] for the different proteins, Table V, show a decrease with increasing molecular weight and size, k_1 for ferritin being 10-fold smaller than k_1 for carbonic anhydrase. In contrast, k_1 calculated from Arve and Liapis [19], shows an increase. Clearly this interaction rate is a reflection of the retention mechanisms dominating adsorption. As different proteins have different sizes, charge distribution and density, this difference is not necessarily

TABLE V

KINETIC PARAMETERS FOR THE ADSORPTION OF PROTEIN TO TRISACRYL M

Protein	k_1 (ml/mol s)		D_p ($\times 10^{-11}$ m^2/s)			
	Eqn. 2	Eqn. 5	Eqn. 2	Eqn. 4	Eqn. 5	Eqn. 3
Carbonic anhydrase	2000	420	7.9	16.2	7.9	14.7
HSA	737	2010	6.1	8.4	6.1	0.90
Ferritin	880	30 800–220 000	3.1	0.3	0.1	0.08

surprising. Similarly high values for the kinetic rates of adsorption have been reported in literature. For example [40], bovine serum albumin adsorbing to the hydrophobic sorbent Hp-70, k_1 was given as 3350 $M^{-1}s^{-1}$, and for IgG binding to the bioaffinity resin [41], Protein A-Lichrospher Si 500, k_1 was 17 000 $M^{-1}s^{-1}$.

(ii) Examination of D_p. Table IV also serves to illustrate the differences in the diffusivities calculated from the various equations. In studies on affinity adsorption, Horstmann *et al.* [16] assumes there is no restriction on the movement of the protein within the particles interior, hence the diffusivities listed are the protein diffusivity in free solution, calculated from a correlation derived from the Stokes–Einstein equation [25], see Table I. The effective diffusivities of HSA as calculated from the model of Tsou and Graham [18] are similar in magnitude to the free diffusivity, that is, although the model is based on pore diffusion, it predicts that the diffusion restrictions are negligible. Assuming that the pore sizes of all of the resins studied are at least an order of magnitude larger than the hydrodynamic radii of HSA, that is, if the molecular cut-off ranges of the resins and the dimensions of the near elipsodal shape of the monomeric albumin molecules [9] are considered, it is likely that the protein effectively diffuses through the porous network at a rate comparable to the rate it diffuses in free solution. These effective diffusivities, calculated from the models of Arnold *et al.* [17] and Tsou and Graham [18] also show a slight concentration dependency. At higher concentrations the protein has less freedom to move about because of the increased number of molecules in solution and also because of possible lateral interactions with increasing amounts of adsorbed protein (the adsorbed protein is likely, also, to hinder accessibility of the free protein into the pores of the resin). These diffusivities also reflect the differences in the performance of the resins, as shown in Figs. 2–8. The value obtained for the Sepharose FF resin is higher than the other resins, and in fact the diffusivity as calculated by the model of Tsou and Graham [18] is twice what it is in free solution. It is important to note here that the standard deviation for the values of D_p shown in Table IV was 30% indicating scatter in the data, possibly due to the heterogeneity of the resin.

Table V lists results of the adsorption behaviour of different proteins to the Trisacryl M resin at a constant concentration. The models of Tsou and Graham [18] and Arnold *et al.* [17] give similarly high estimates of the diffusivity of carbonic anhydrase, and low estimates for the largest protein ferritin, whilst the model of Arve and Liapis [19] also predicts that there is no restriction to movement of the small proteins, and that the pore diffusion of ferritin is 1/40th that of the free diffusivity. Similar phenomena of pore restrictions resulting in low diffusivities has been repeatedly reported in affinity [28,33], reversed-phase [31,42] and ion-exchange chromatography [17,18,30,33,43,44]. The molecular quantification of this phenomenon still requires systematic description if the full predictive capabilities of adsorption models are to routinely aid process scale-up in ion-exchange chromatography.

CONCLUSIONS

The adsorption of proteins to ion-exchange sorbents is a complex process that has yet to be well defined in terms of molecular kinetic mechanisms. From a physical and chemical viewpoint, it is known that electrostatic forces steer the protein towards the charged resin, yet other associated forces, for example hydrophobic interactions,

may also be contributing factors. It has been shown that if the pores of the resin are typically of the same order of magnitude as the diffusing protein [33], then they will restrict mass transfer and adsorption, the ramifications of which may be a low capacity and/or slow kinetics. Furthermore, it can be postulated that molecular docking, protein masking and multiple and dynamic orientation of protein isoforms may effect the efficiency of the process in terms of purity levels and throughput. Interpretation of these non-ideal, non-equilibrium phenomena from observed adsorption behaviour is a taxing task. Most mathematical models derived to predict true adsorption behaviour, have neglected these detrimental effects because of the complexity of the associated mass balance equations. Indeed no analytical solution to even the idealised mass balance equation of eqn. 5 has been forthcoming.

The results presented here, however, have provided further insight into the validity of the various models outlined in the theory section. Firstly, the Langmuir isotherm, although a very poor fit to the high affinity ion-exchange process, yields useful qualitative information about the association constants and the protein capacities. Variation between different anion resins with the same functional group can be seen through the association constant, which also shows protein size dependency. The maximum capacity of each resin studied has also been shown, via the Langmuir treatment to be dependent on the hydrodynamic size of the protein. Secondly, the kinetic equations, although derived using different assumptions, indicate conclusively, that there were no restrictions to the diffusion of the small proteins such as carbonic anhydrase, upon binding to each of the resins examined; the extracted values for the effective diffusivities were of the same order of magnitude as the correlated free diffusivity. Adsorption of the largest protein, ferritin, was found to be pore restricted, with the diffusivity calculated using the models of Tsou and Graham [18], Arnold et al. [17] and Arve and Liapis [19] being up to 1/40th that in solution. With the use of the models of Horstmann et al. [16] and Arve and Liapis [19], no definite trend was apparent for the values of the rate of interaction for the protein binding to the charged functional groups. The model of Arve and Liapis [19] gave rate values that were independent of concentration, high for large proteins and low for smaller proteins. The model of Horstmann et al. [16], on the contrary, yielded lower rates at higher concentrations, and higher rates for the smallest protein. All the rates extracted from this model were also lower than those predicted from the model of Arve and Liapis [19]. The values for these experimentally and theoretically derived parameters, q_m, K_a, D_p and k_1, concur well with those reported in the literature [14,16–19,28,33]. High protein capacity and high association constant are indicative of ion-exchange adsorption, whilst the kinetic parameters, D_p and k_1 correlate well considering the ratio of protein to pore size.

The applicability of these data in preparative scale-up, has yet to be ascertained, where the equilibrium isotherm is unlikely to be linear, and operation will invariably be at high protein concentrations, at the saturation level of the isotherm. The premise of Langmuir behaviour is also dubious. Furthermore, the assumptions of restricted pore diffusion events or kinetic rate dominance are unlikely to be valid, whilst protein–protein and protein–ion interactions are anticipated to be far more complex than what occurs in these batch experiments. The experiments in the study have been performed with pure protein solutions, and in a batch mode of operation. In preparative chromatography, packed column configuration is usually adopted and the feed stock

is a cocktail of proteins, each varying in their abundance, charge distribution, size and sorption behaviour. In addition, heterogeneity of the resins in terms of particle to pore size and ligand distribution may become more pronounced in preparative operation, and this heterogeneity will require attention during optimization and prediction studies. Details of such practical and modelling applications with packed beds will be reported subsequently.

SYMBOLS

a^2 $b^2 - \dfrac{C_0 V}{q_m v}$

b $\dfrac{1}{2}\left[C_0\left(\dfrac{v}{V}\right) + q_m + K_d\left(\dfrac{v}{V}\right)\right]$

C_0 initial protein concentration in the bulk fluid

$C(t)$ concentration of protein at any time, t

c^* equilibrium concentration of protein in solution

D_p effective (pore) diffusivity

e batch void fraction

e_p porosity of the resin

$F(t)$ fractional obtainment to equilibrium, $\dfrac{q^* - q(t)}{q^* - q_0}$

K overall mass transfer coefficient

k_1 the first order rate constant, forward rate constant

k_2 the reverse rate constant

K_a the association constant, $\dfrac{k_1}{k_2}$

K_d the dissociation constant, $\dfrac{1}{K_a}$

m'' $\dfrac{q^* - q(t)}{C(t) - C_0}$

q_m maximum protein capacity of the resin

q_0 initial concentration of protein adsorbed to the resin

$q(t)$ concentration of protein adsorbed at any time t

q^* concentration of protein adsorbed to the resin in equilibrium with c^*

r_p radius of resin particle

V volume of buffer in the bath

v volume of resin

α $\begin{cases} (\gamma - 1)^{1/3} & \gamma > 1 \\ 0 & \gamma = 1 \\ -(1 - \gamma)^{1/3} & \gamma < 1 \end{cases}$

γ $\dfrac{e\, C_0}{q_0\, r_p}$

ω $\left[1 - \gamma\left(1 - \dfrac{C(t)}{C_0}\right)\right]^{1/3}$

REFERENCES

1 J. Saint-Blanchard, J. M. Kirzin, P. Riberon, F. Deht, J. Fourcant, P. Girot and E. Boschett, in T. C. J. Gribnau, J. Visse and R. J. F. Nivard (Editors), *Affinity Chromatography and Related Techniques*, Elsevier, Amsterdam, 1982, pp. 200–300.
2 S. M. Wheelwright, *Bio/Technology*, 5 (1987) 789.
3 M. T. W. Hearn, in J. A. Asenjo (Editor), *Isolation and Purification Separation Processes in Biotechnology*, Marcel Decker, New York, 1990, pp. 17–66.
4 J. Luiken, R. Van der Zee and G. W. Welling, *J. Chromatogr.*, 284 (1984) 482.
5 M. T. W. Hearn, A. N. Hodder, P. G. Stanton and M. I. Aguilar, *Chromatographia*, 24 (1987) 769.
6 F. E. Regnier, *Science (Washington, D.C.)*, 238 (1987) 317.
7 P. Oroszlan, R. Blanco. X.-M. Lu, D. Yarmush and B. L. Karger, *J. Chromatogr.*, 500 (1990) 481.
8 S. Mazsaroff, S. Cook and F. E. Regnier, *J. Chromatogr.*, 443 (1988) 119.
9 P. G. Squire, P. Moser and C. T. O. Konski, *Biochemistry*, 7 (1968) 4261.
10 P. Strop, V. Zizkovsky, J. Korcakova, M. Havranova and F. Mikes, *Int. J. Biochem.*, 16 (1984) 805.
11 M. T. W. Hearn, A. N. Hodder and M. I. Aguilar, *J. Chromatogr.*, 327 (1985) 47.
12 B. J. Horstmann and H. A. Chase, *Chem. Eng. Res. Des.*, 67 (1989) 243.
13 H. A. Chase, *J. Chromatogr.*, 297 (1984) 179.
14 F. B. Anspach, A. Johnston, H.-J. Wirth, K. K. Unger and M. T. W. Hearn, *J. Chromatogr.*, 499 (1990) 103.
15 B. L. Yang, M. Goto and S. Goto, *J. Chem. Eng. Japan*, 22 (1989) 532.
16 B. J. Horstmann, C. N. Kenney and H. A. Chase, *J. Chromatogr.*, 361 (1986) 179.
17 F. H. Arnold, H. W. Blanche and C. R. Wilke, *Chem. Eng. J.*, 30 (1985) B9.
18 H. S. Tsou and E. E. Graham, *AIChE J.*, 31 (1985) 1959.
19 B. H. Arve and A. I. Liapis, *AIChE J.*, 33 (1987) 179.
20 C. Delisi, H. W. Hethcote and J. W. Brettler, *J. Chromatogr.*, 240 (1982) 283.
21 R. D. Fleck, D. J. Kirwan and K. R. Hall, *Ind. Eng. Fundam.*, 12 (1973) 95.
22 G. H. Cowan, I. S. Gosling, J. F. Laws and W. P. Sweetenham, *J. Chromatogr.*, 363 (1986) 37.
23 S. C. Nigam and H. Y. Wang, in J. A. Asenjo and J. Hong (Editors), *Separations, Purification and Recovery in Biotechnology: Recent Advances and Mathematical Modeling. (ACS Symposium Series*, No. 314), American Chemical Society, Washington, DC, 1986, pp. 153–168.
24 H. Ohashi, T. Sugawar, K. Kikuchi and K. Konno, *J. Chem. Eng. Japan*, 14 (1981) 433.
25 M. E. Young, P. A. Carroad and R. L. Bell, *Biotech. Bioeng.*, 12 (1980) 947.
26 R. C. Travers and F. C. Church, *Int. J. Peptide Prot. Res.*, 26 (1985) 539.
27 Y. Kato, K. Nakamura and T. Hashimo, *J. Chromatogr.*, 253 (1982) 219.
28 F. B. Anspach, A. Johnston, H.-J. Wirth, K. K. Unger and M. T. W. Hearn, *J. Chromatogr.*, 476 (1989) 205.
29 R. Janzen, K. K. Unger, W. Muller and M. T. W. Hearn, *J. Chromatogr.*, 522 (1990) 77.
30 E. E. Graham and C. F. Fook, *AIChE J.*, 28 (1982) 245.
31 W. Kopaciewicz, S. Fulton and S. Y. Lee, *J. Chromatogr.*, 409 (1987) 111.
32 B. F. Ghrist, M. A. Stadalius and L. R. Snyder, *J. Chromatogr.*, 387 (1987) 1.
33 A. Johnston and M. T. W. Hearn, *J. Chromatogr.*, 512 (1990) 101.
34 A. Fersht, in A. Fersht (Editor), *Enzyme Structure and Mechanism*, W. H. Freeman, Reading, UK, 1977, pp. 130–131.
35 M. I. Aguilar, A. N. Hodder and M. T. W. Hearn, *J. Chromatogr.*, 327 (1984) 115.
36 N. K. Boardman and S. M. Partridge, *Biochem. J.*, 59 (1955) 543.
37 R. A. Barford, B. J. Sliwinski and H. L. Rothbart, *J. Chromatogr.*, 185 (1979) 393.
38 W. Kopaciewicz, M. A. Rounds, J. Fausnaught and F. E. Regnier, *J. Chromatogr.*, 266 (1983) 3.
39 M. A. Rounds and F. E. Regnier, *J. Chromatogr.*, 283 (1984) 37.
40 K. Nakamura, Y. Hirai, H. Kitana and N. Ise, *Biotech. Bioeng.*, 30 (1987) 216.
41 D. S. Hage and R. R. Walter, *Anal. Biochem.*, 58 (1986) 274.
42 C. K. Colton, G. N. Satterfield and C. J. Lai, *AIChE J.*, 21 (1975) 289.
43 K. Yamamoto, R. Nakanishi, R. Matsuno and T. Kamikubo, *Biotech./Bioeng.*, 225 (1983) 1465.
44 E. Furuya, Y. Takeuchi and K. E. Noll, *J. Chem. Eng. Japan*, 22 (1989) 670.
45 Q. M. Mao, A. Johnston, I. Prince and M. T. W. Hearn, *J. Chromatogr.*, 548 (1991) 147.